SIMULATION OF REAL AERODYNASMICS PROBLEMS USING HIGHER-ACCURACY LOWER-COST SCHEME ON UNSTRUCTURED MESHES

Ilya ABALAKIN, Pavel BAKHVALOV, Vladimir BOBKOV, Alexey DUBEN, and Tatiana KOZUBSKAYA

Keldysh Institute of Applied Mathematics RAS, Moscow

Outline

- Introduction
  - EBR and WENO-EBR Schemes
  - In-House Code NOISEtte
  - Verification
  - Simulations

For solving real aerodynamics problems we need:

1) **high accuracy** (enough for engineering);
2) efficient **shock capturing techniques**;
3) efficient scalable **parallel algorithms**;
4) reasonable computational **costs**.

These items are **interdependent** and should be developed **all in the same boat**

We try to do this under the condition of **unstructured meshes**
well suitable for the problems with complex geometry, typical for applications

Introduction

EBR and WENO-EBR Schemes

In-House Code NOISEtte

Verification

Simulations

EBR (Edge-Based Reconstruction) Schemes =

vertex-centered schemes
based on **quasi-1D edge-oriented reconstruction** of variables
for **unstructured** meshes

1. Dervieux, A. and Debiez, C. Mixed element volume MUSCL methods with weak viscosity for steady and unsteady flow calculation. *Computer and Fluids* 29: 89-118, **1999**

2. Gourvitch, N., G. Rogé, I. Abalakin, A. Dervieux and T. Kozubskaya. A tetrahedral-based superconvergent scheme for aeroacoustics. *INRIA Report* 5212, **2004**

3. Abalakin, I., A. Dervieux and T. Kozubskaya. High Accuracy Finite Volume Method for Solving Nonlinear Aeroacoustics Problems on Unstructured Meshes. *Chinese Journal of Aeroanautics* 19: 97-104, **2006**

4. Koobus, B., F. Alauzet and A. Dervieux. Numerical algorithms for unstructured meshes, In: *Computational Fluid Dynamics*, edited by F. Magoulès, London, New-York: CRC Press, **2011**, p.131-203

5. Ilya Abalakin, Pavel Bakhvalov, Tatiana Kozubskaya. Edge-Based Methods in CAA. – In *"Accurate and Efficient Aeroacoustic Prediction Approaches for Airframe Noise",* Lecture Series 2013-03, Ed. by C.Schram, R.Denos, E.Lecomte, von Karman Institute for Fluid Dynamics, **2013** (ISBN-13 978-2-87516-048-5)

6. Ilya Abalakin, Pavel Bakhvalov and Tatiana Kozubskaya. Edge-based reconstruction schemes for prediction of near field flow region in complex aeroacoustic problems, *International Journal of Aeroacoustics*, Vol.13, N 3&4, **2014**, p. 207-234

- **Triangular** and **tetrahedral meshes,** although extension to **hybrid meshes** has been done
- **Method of lines** for solving PDE
- **Vertex-centered formulation**

Node i is a center of cell of volume V_i

All the geometrical work (search for neighbors of 1st and 2nd levels, construction of cells, faces and normals, stencils, …) is performed only once, at the preprocessing stage

- **Conservation laws**

result from the general formulation:

$$\boxed{\left[\frac{\partial \mathbf{Q}}{\partial t}\right]_i + \frac{1}{V_i}\sum_{j\in N(i)} \mathcal{F}_{ij} S_{ij} = 0}$$

$N(i)$ – a set of faces of cell i containing node i (i.e. a set of edges going out of node i)

$\mathcal{F}_{ij}$ — flux through the cell face ij of square S_{ij} (projected to the normal of cell i)

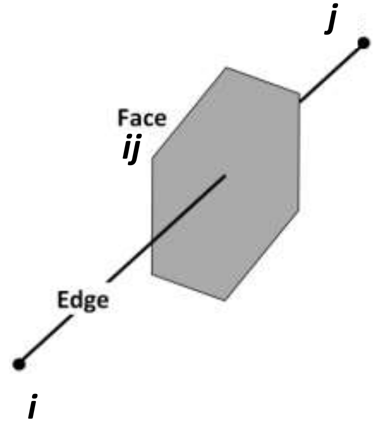

- **Edge-wise implementation:**

The main loop – on edges with accumulating necessary integral sums in nodes

The scheme construction is reduced to the problem:

how to determine the fluxes $\mathcal{F}_{ij}$ **=???**

Riemann Solvers

Important remark:

Define the flux $\mathcal{F}_{ij}$ through each face
in a single point = midpoint of corresponding edge (i.e. the edge intersecting this face)

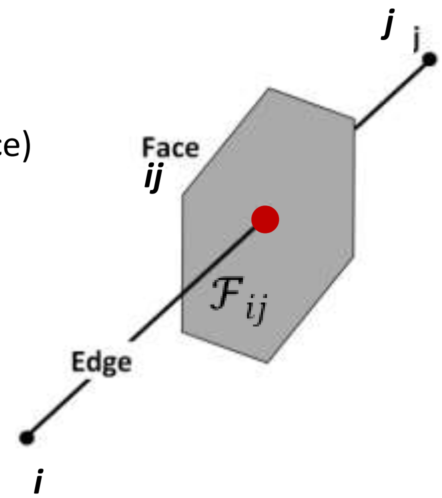

$$\mathcal{F}_{ij} = h\left(\mathbf{Q}_{ij}^{L}, \mathbf{Q}_{ij}^{R}\right) = \frac{\mathbf{F}\left(\mathbf{Q}_{ij}^{L}\right) + \mathbf{F}\left(\mathbf{Q}_{ij}^{R}\right)}{2} - \frac{\delta}{2}\left|\mathbf{A}_{ij}\right|\left(\mathbf{Q}_{ij}^{R} - \mathbf{Q}_{ij}^{L}\right)$$ **Roe**

$$\mathcal{F}_{ij} = h\left(\mathbf{F}_{ij}^{L}, \mathbf{F}_{ij}^{R}, \mathbf{Q}_{i}, \mathbf{Q}_{j}\right) = \frac{\mathbf{F}_{ij}^{L} + \mathbf{F}_{ij}^{R}}{2} - \frac{\delta}{2}\operatorname{sign}\mathbf{A}_{ij}\left(\mathbf{Q}_{i}, \mathbf{Q}_{j}\right)\left(\mathbf{F}_{ij}^{R} - \mathbf{F}_{ij}^{L}\right)$$ **Huang**

$$\mathcal{F}_{ij} = h\left(\mathbf{F}_{ij}^{L}, \mathbf{F}_{ij}^{R}, \mathbf{Q}_{i}, \mathbf{Q}_{j}, \mathbf{Q}_{ij}^{L}, \mathbf{Q}_{ij}^{R}\right) = \frac{\mathbf{F}_{ij}^{L} + \mathbf{F}_{ij}^{R}}{2} - \frac{\delta}{2}\left|\mathbf{A}\left(\mathbf{Q}_{i}, \mathbf{Q}_{j}\right)\right|_{ij}\left(\mathbf{Q}_{ij}^{R} - \mathbf{Q}_{ij}^{L}\right)$$ **Hybrid**

$$\mathcal{F}_{ij} = \left(\mathbf{F}^{+}\right)_{ij}^{L} + \left(\mathbf{F}^{-}\right)_{ij}^{R}, \quad \mathbf{F} = \mathbf{F}^{+} + \mathbf{F}^{-}$$ **Flux splitting methods**

$(\bullet)^{L/R}$ — reconstruction of mesh function from the left (L) or from the right (R) of cell face

$$\mathbf{F} = \mathbf{F}_{x} n_{x} + \mathbf{F}_{y} n_{y} + \mathbf{F}_{z} n_{z}, \qquad \mathbf{A} = \frac{\partial \mathbf{F}}{\partial \mathbf{Q}} = \mathbf{S}\Lambda\mathbf{S}^{-1}$$

Note, if $(\bullet)^{L} = (\bullet)^{R} = ((\bullet)_{i} + (\bullet)_{j})/2$
we obtain the 2nd-order vertex-centered (Gauss-Green) scheme for barycentric cells

If we like to gain **more accuracy** we should define the reconstructed variables
$(\bullet)^{L}$ = ??? and **$(\bullet)^{R}$ = ???**

EBR and WENO-EBR Schemes

Stencil of Quasi-1D Reconstruction

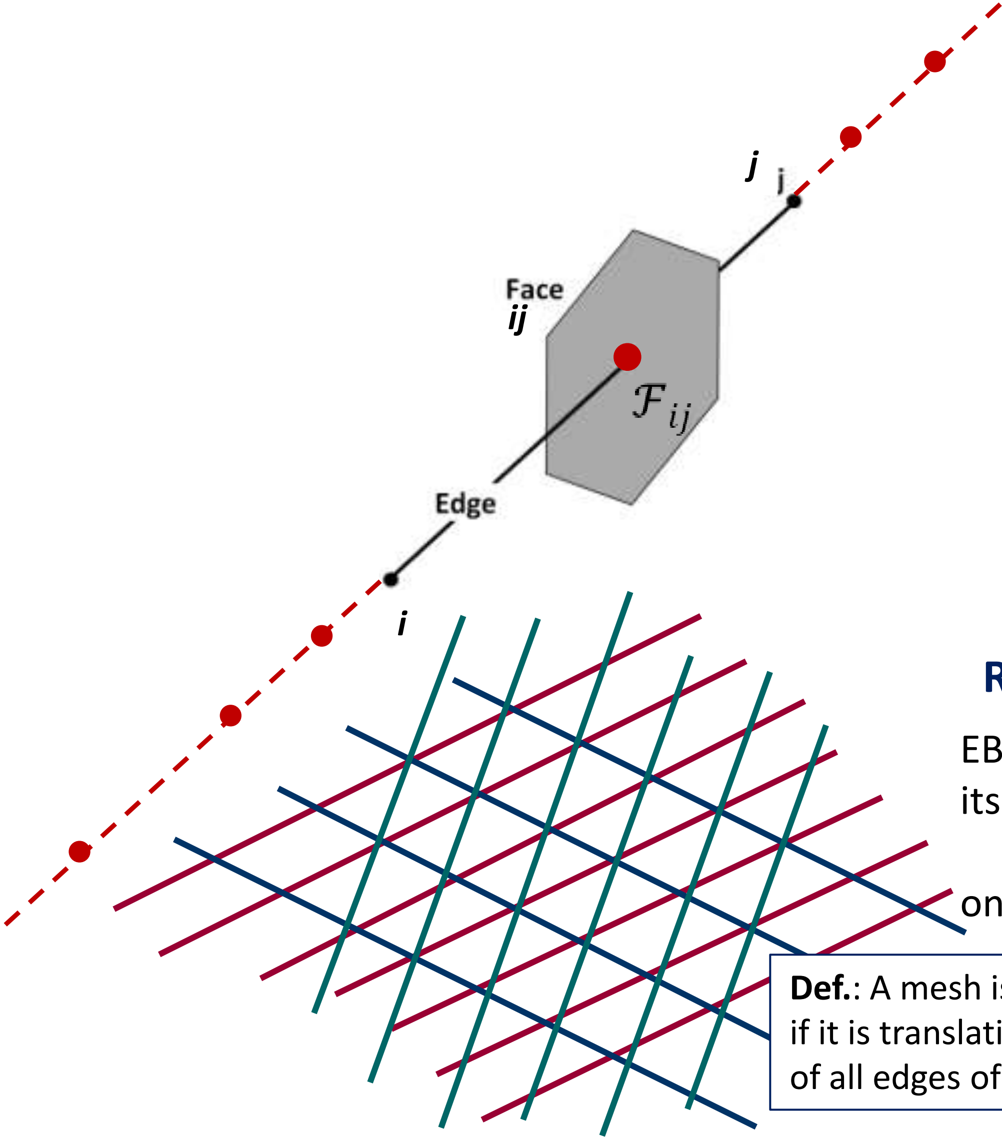

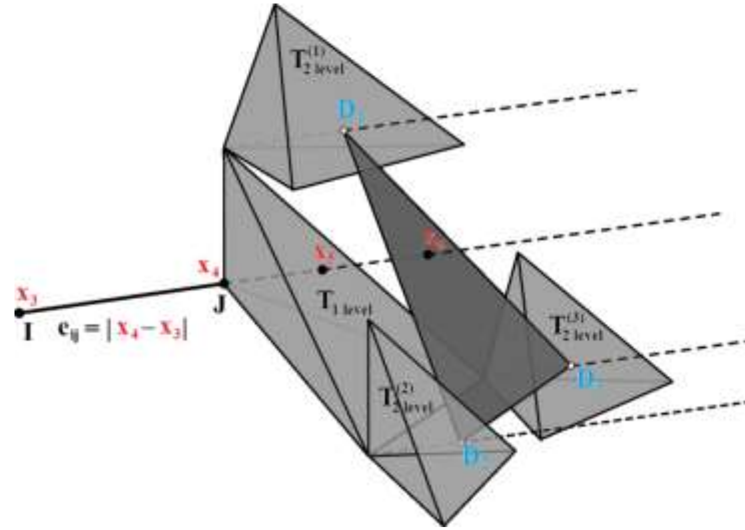

One of the possible ways how to define
the stencil points on the edge-based direction
The values are found using **linear interpolations**

Requirement to the stencil choice:

EBR schemes **must** reach
its **highest** theoretically possible **order**
(the **5th-6th order**)
on **TS-meshes** (translationally-symmetric meshes)

Def.: A mesh is said to be **translationally symmetric**
if it is translationally invariant with respect to the vectors
of all edges of the mesh

Quasi-1D Reconstruction

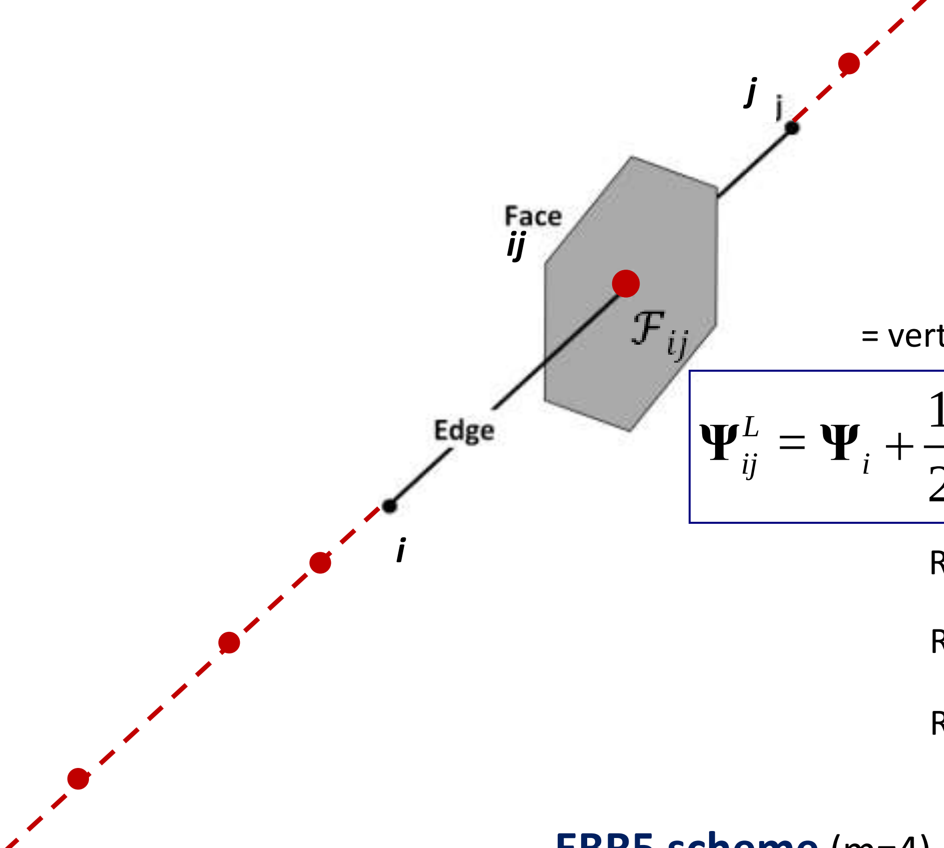

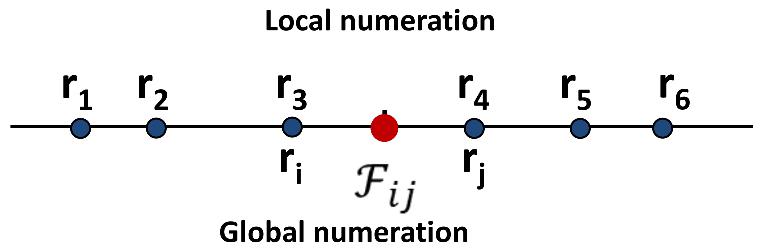

Reconstruction of vector variable $\mathbf{\Psi}$

= vertex value + linear combination of differences $\Delta\mathbf{\Psi}_{k+1/2} = \mathbf{\Psi}_{k+1} - \mathbf{\Psi}_k$

$$\boxed{\mathbf{\Psi}_{ij}^{L} = \mathbf{\Psi}_i + \frac{1}{2}\sum_{k=1}^{m}\beta_{ij,k}^{L}\Delta\mathbf{\Psi}_{k+1/2}, \quad \mathbf{\Psi}_{ij}^{R} = \mathbf{\Psi}_j - \frac{1}{2}\sum_{k=1}^{m}\beta_{ij,k}^{R}\Delta\mathbf{\Psi}_{k+1/2}}$$

Reconstruction of conservative variables $\mathbf{\Psi}_{ij}^{L/R} = \mathbf{Q}_{ij}^{L/R}$

Reconstruction of flux variables $\mathbf{\Psi}_{ij}^{L/R} = \mathbf{F}_{ij}^{L/R}$

Reconstruction of physical variables $\mathbf{\Psi}_{ij}^{L/R} = \mathbf{Q}\left(\mathbf{U}_{ij}^{L/R}\right)$

EBR5 scheme (m=4)

$$\beta_{ij,1}^{L} = -\frac{1}{15}\frac{\Delta r_{7/2}}{\Delta r_{3/2}}, \quad \beta_{ij,2}^{L} = \frac{11}{30}\frac{\Delta r_{7/2}}{\Delta r_{5/2}}, \quad \beta_{ij,3}^{L} = \frac{4}{5}\frac{\Delta r_{7/2}}{\Delta r_{7/2}}, \quad \beta_{ij,4}^{L} = -\frac{1}{10}\frac{\Delta r_{7/2}}{\Delta r_{9/2}}$$

$$\beta_{ij,1}^{R} = -\frac{1}{10}\frac{\Delta r_{7/2}}{\Delta r_{5/2}}, \quad \beta_{ij,2}^{R} = \frac{4}{5}\frac{\Delta r_{7/2}}{\Delta r_{7/2}}, \quad \beta_{ij,3}^{R} = \frac{11}{30}\frac{\Delta r_{7/2}}{\Delta r_{9/2}}, \quad \beta_{ij,4}^{R} = -\frac{1}{15}\frac{\Delta r_{7/2}}{\Delta r_{11/2}}$$

EBR3 scheme (m=2)

$$\beta_{ij,1}^{L} = \frac{1}{3}\frac{\Delta r_{7/2}}{\Delta r_{5/2}}, \quad \beta_{ij,2}^{L} = \frac{2}{3}\frac{\Delta r_{7/2}}{\Delta r_{7/2}}$$

$$\beta_{ij,1}^{R} = \frac{2}{3}\frac{\Delta r_{7/2}}{\Delta r_{7/2}}, \quad \beta_{ij,2}^{R} = \frac{1}{3}\frac{\Delta r_{7/2}}{\Delta r_{9/2}}$$

EBR and WENO-EBR Schemes

WENO-EBR scheme (for *L*-reconstruction – from the left)

- On the 5-points stencil we can build **three** *L*-reconstructions of the 2nd-order (m=2). Apply them to characteristics variables $\left[\mathbf{S}^{-1}\mathbf{Q}\right]_{ij}$

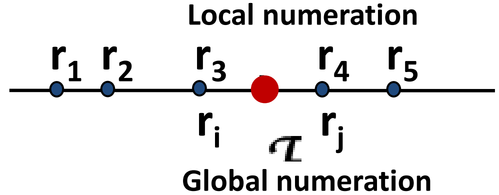

$$\mathcal{L}_{ij}^{L(1)} = \mathbf{S}_{ij}^{-1}\mathbf{Q}_i + \mathbf{S}_{ij}^{-1}\frac{\Delta r_{7/2}}{2}\left(-\frac{1}{3}\frac{\Delta\mathbf{Q}_{3/2}}{\Delta r_{3/2}} + \frac{5}{3}\frac{\Delta\mathbf{Q}_{5/2}}{\Delta r_{5/2}}\right) = \mathbf{S}_{ij}^{-1}\mathbf{Q}_i + SlopeL(1)$$

$$\mathcal{L}_{ij}^{L(2)} = \mathbf{S}_{ij}^{-1}\mathbf{Q}_i + \mathbf{S}_{ij}^{-1}\frac{\Delta r_{7/2}}{2}\left(\frac{1}{3}\frac{\Delta\mathbf{Q}_{5/2}}{\Delta r_{5/2}} + \frac{2}{3}\frac{\Delta\mathbf{Q}_{7/2}}{\Delta r_{7/2}}\right) = \mathbf{S}_{ij}^{-1}\mathbf{Q}_i + SlopeL(2)$$

$$\mathcal{L}_{ij}^{L(3)} = \mathbf{S}_{ij}^{-1}\mathbf{Q}_i + \mathbf{S}_{ij}^{-1}\frac{\Delta r_{7/2}}{2}\left(\frac{4}{3}\frac{\Delta\mathbf{Q}_{7/2}}{\Delta r_{7/2}} - \frac{1}{3}\frac{\Delta\mathbf{Q}_{9/2}}{\Delta r_{9/2}}\right) = \mathbf{S}_{ij}^{-1}\mathbf{Q}_i + SlopeL(3) \qquad \mathbf{S}_{ij}^{-1} = \mathbf{S}_{ij}^{-1}\left(\mathbf{Q}_i, \mathbf{Q}_j\right)$$

- Weighted combination of three reconstructions in accordance to classical **FD WENO method** *(Shu, 1994)*

$$\mathcal{L}_{ij}^{L} = \sum_{k=1}^{3}\omega_k^L \mathcal{L}_{ij}^{L(k)}, \quad \omega_k^L = \frac{\sigma_k^L}{\sigma_1^L + \sigma_2^L + \sigma_3^L} \quad \sigma_k^L = \frac{\Omega^{(k)}}{\left(10^{-10} + IS_k^L\right)^2} \quad \Omega^{(1)} = \frac{1}{10} \quad \Omega^{(2)} = \frac{6}{10} \quad \Omega^{(3)} = \frac{3}{10}$$

"Smoothness monitors"

$$IS_1^L = \frac{13}{12}\left(\mathbf{S}_{ij}^{-1}\Delta\mathbf{Q}_{5/2} - \mathbf{S}_{ij}^{-1}\Delta\mathbf{Q}_{3/2}\right)^2 + \frac{1}{4}\left(3\mathbf{S}_{ij}^{-1}\Delta\mathbf{Q}_{5/2} - \mathbf{S}_{ij}^{-1}\Delta\mathbf{Q}_{3/2}\right)^2$$

$$IS_2^L = \frac{13}{12}\left(\mathbf{S}_{ij}^{-1}\Delta\mathbf{Q}_{7/2} - \mathbf{S}_{ij}^{-1}\Delta\mathbf{Q}_{5/2}\right)^2 + \frac{1}{4}\left(\mathbf{S}_{ij}^{-1}\Delta\mathbf{Q}_{7/2} + \mathbf{S}_{ij}^{-1}\Delta\mathbf{Q}_{5/2}\right)^2$$

$$IS_3^L = \frac{13}{12}\left(\mathbf{S}_{ij}^{-1}\Delta\mathbf{Q}_{9/2} - \mathbf{S}_{ij}^{-1}\Delta\mathbf{Q}_{7/2}\right)^2 + \frac{1}{4}\left(\mathbf{S}_{ij}^{-1}\Delta\mathbf{Q}_{9/2} - 3\mathbf{S}_{ij}^{-1}\Delta\mathbf{Q}_{7/2}\right)^2$$

- Reconstruction of conservative variables

$$\left.\begin{aligned} \mathbf{Q}_{ij}^L &= \mathbf{S}_{ij}\mathcal{L}_{ij}^L = \mathbf{Q}_i + \mathbf{S}_{ij}\sum_{k=1}^{3}\omega_k^L\, SlopeL(k) \\ \mathbf{Q}_{ij}^R &= \mathbf{S}_{ij}\mathcal{L}_{ij}^R = \mathbf{Q}_j - \mathbf{S}_{ij}\sum_{k=1}^{3}\omega_k^R\, SlopeR(k) \end{aligned}\right\} \xrightarrow{\text{Riemann solver}} h\left(\mathbf{Q}_{ij}^L, \mathbf{Q}_{ij}^R\right)$$

Characteristic Quasi-FD WENO approach => WENO-EBR Scheme

Introduction

EBR and WENO-EBR Schemes

In-House Code NOISEtte

Verification

Simulations

Meshes
- unstructured meshes;
- barycentric (median) and orthocentric (CCS) control volumes

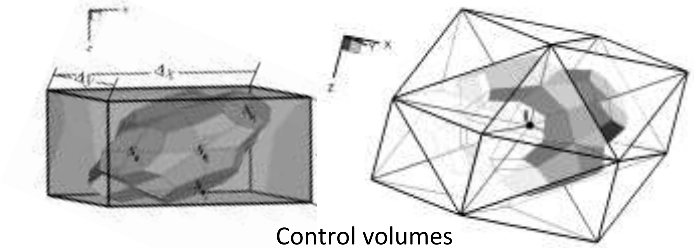
Control volumes

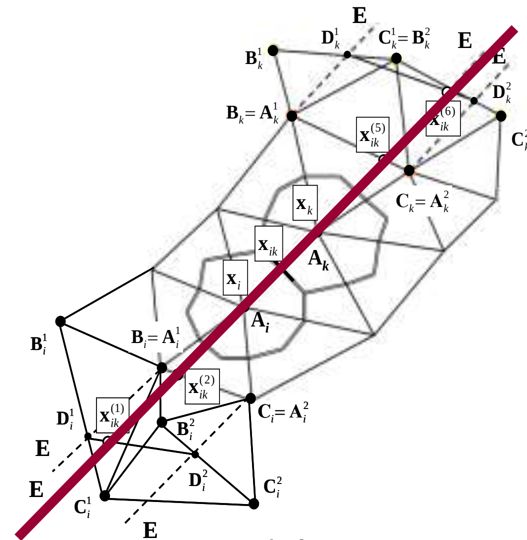

2D stencil of reconstruction

Basic mathematical model – full compressible Navier-Stokes equations
- 1eq Spalart-Allmaras turbulence model
- 2eq k-ε, k-ω, Menter SST

Approaches:
- Direct Numerical Simulation (DNS)
- (U)RANS, PANS
- LES (Smagorinsky, WALE, σ, …)
- Nonzonal hybrid RANS-LES: (I)DDES

Numerical methods:
- space discretization: vertex-centered higher-accuracy EBR schemes (up to 6th),
- WENO/TVD-EBR techniques
- time integration: explicit Runge-Kutta 3-4 order scheme and implicit 1-2 order scheme (BiCGSTAB solver for SLAE)

High efficiency MPI+OpenMP parallelization
- large scale computations using meshes up to 10^9 cells and up to 10^5 CPUs
- parallel tools for pre and post processing

Far field acoustics: FWH method

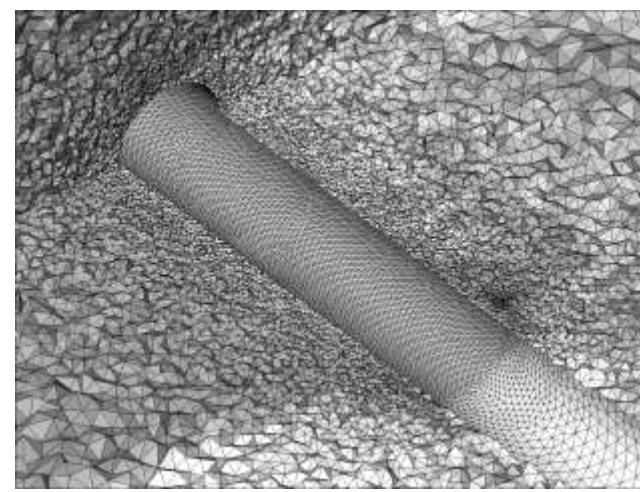
Unstructured mesh

Speed-up of MPI+OpenMP parallelization

Mesh: 16M nodes, 100M tetrahedra

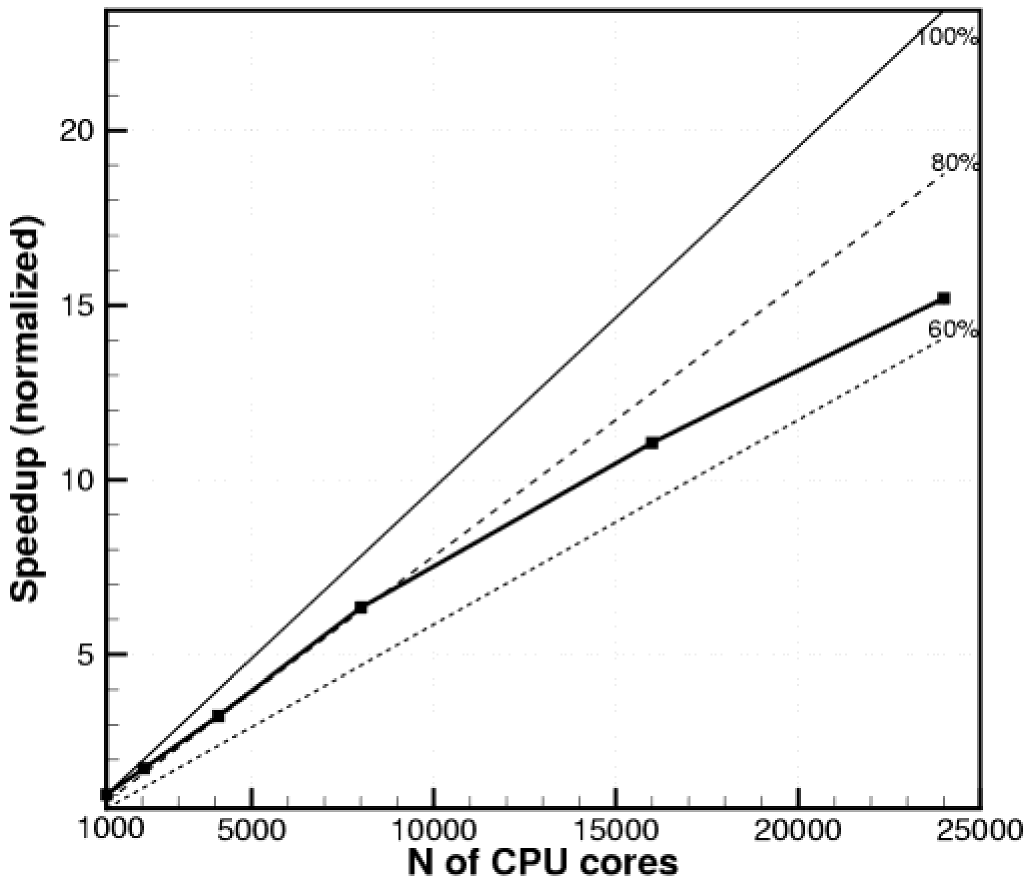

Introduction

EBR and WENO-EBR Schemes

In-House Code NOISEtte

Verification

Simulations

Verification

- Algorithms realized in NOISEtte are verified on a large amount of test cases
- Results of verification on canonical turbulent flows will be presented here

Test case #1: Decay of isotropic homogenous turbulence

Objective: calibration of empirical constants of LES, DES models

Experiment: Comte-Bellot&Corrsin, 1971

Flow parameters: Re=1620

Meshes: 32^3, 64^3 Models: LES, DES

Initial field: generated u,v,w from E(k) at T=0

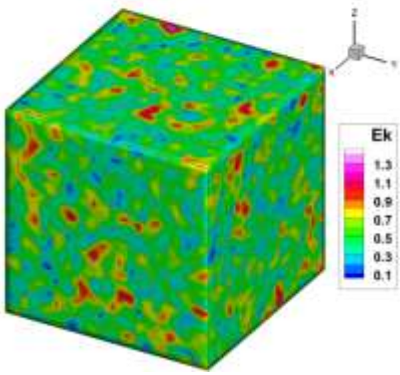

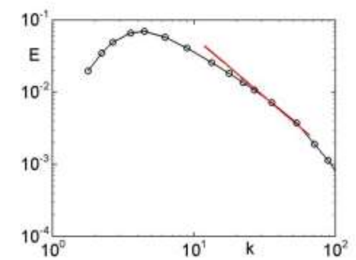

Calibration of C_{DES} constant:

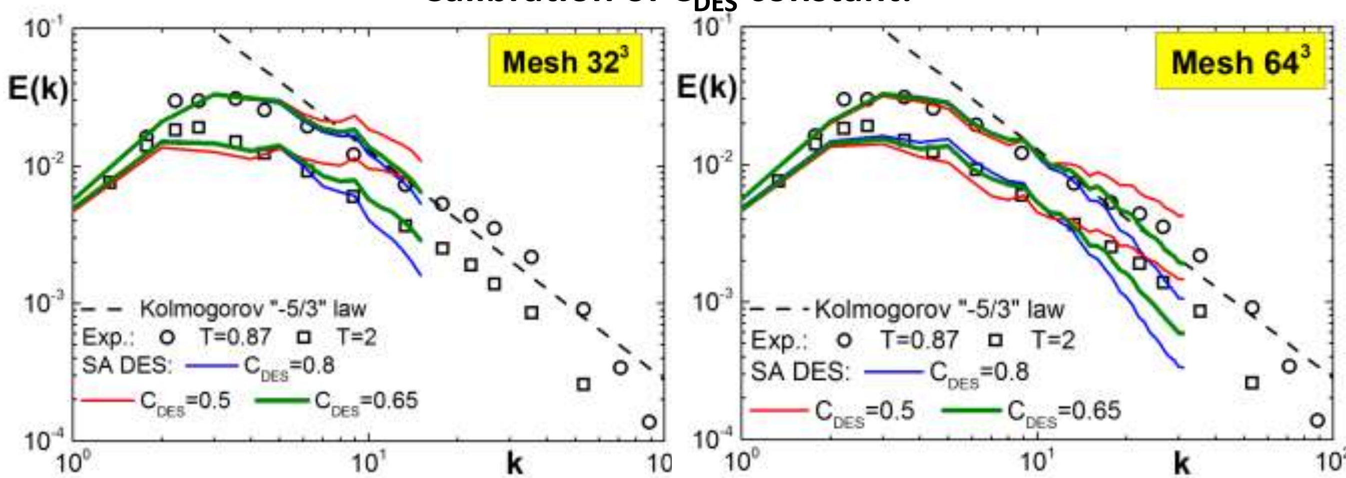

Verification

Test case #2: Turbulent planar channel flow

Objective: verification of WMLES branch of IDDES

Comparison: DNS by Jimenez et. al

Flow parameters: $\mathrm{Re}_\tau = 0.5 \cdot H \cdot u_\tau / \nu = 400$

$\mathrm{Re}_b = 1.4 \cdot 10^4$

Periodic on X and Z direction

Source term x pressure gradient to keep bulk velocity

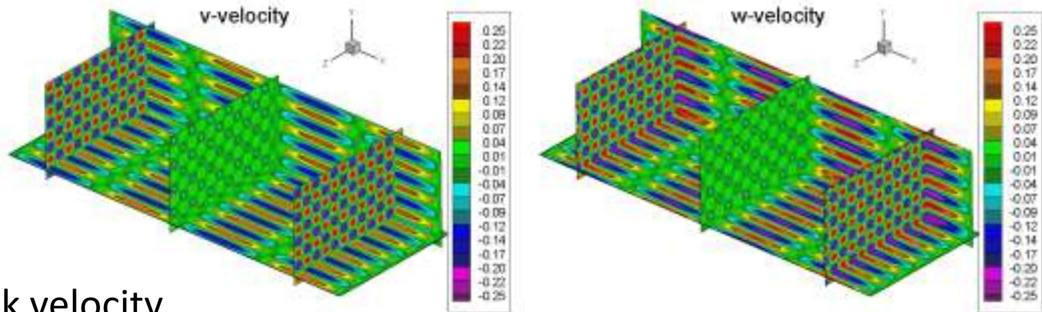

Initial fields for v and w velocities, u=1 in entire domain

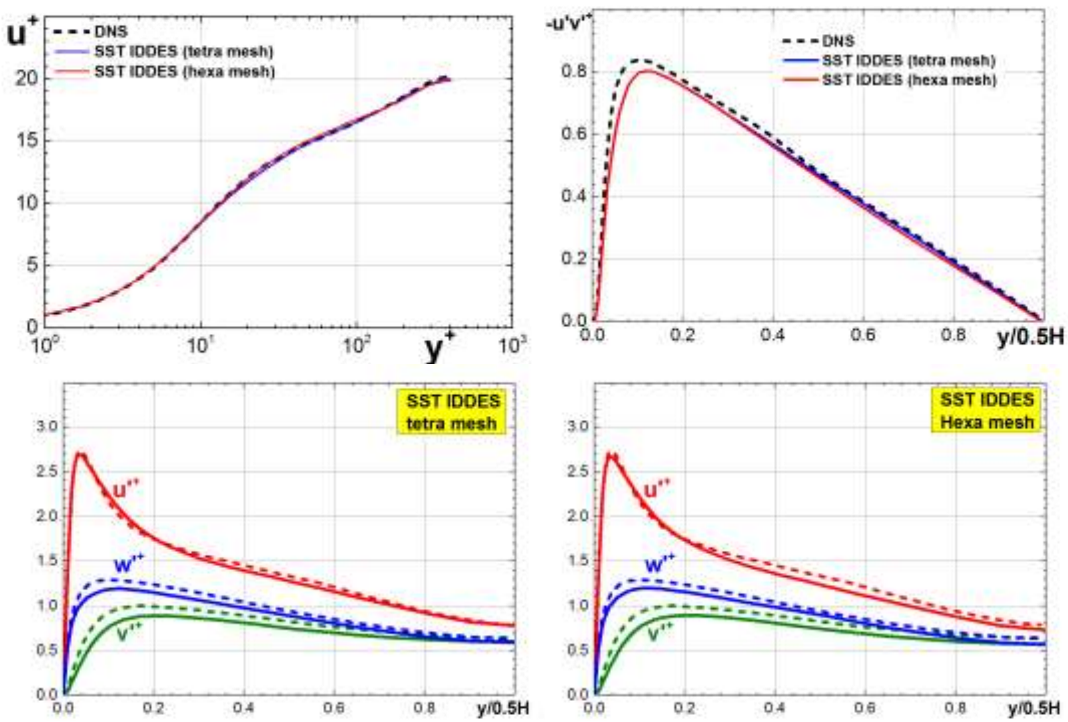

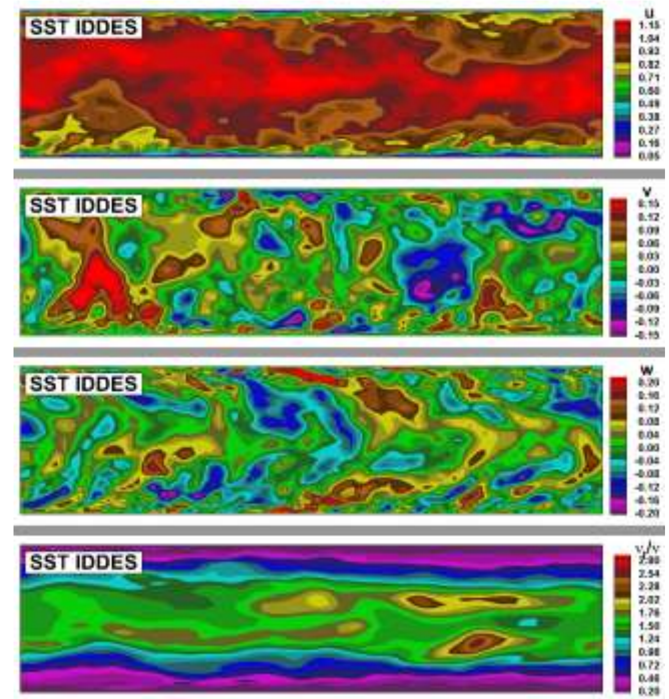

Test case #3: Turbulent flow in channel with back facing step

Objective: to test DDES approach

Flow parameters: Re=28000 (H=3.8 см, U_0=11.3 м/с (M=0.033)

Experimental data: Vogel & Eaton 1985

Computational domain:

Spanwise (Z) direction: periodicity, L_z=2H

Mesh: 0.74M nodes, 4.2M tetrahedrons. $\Delta z = H/10$

Input BC: fixed velocity u and turbulent viscosity profiles (based on Θ=0.123H)

Numerical setup:

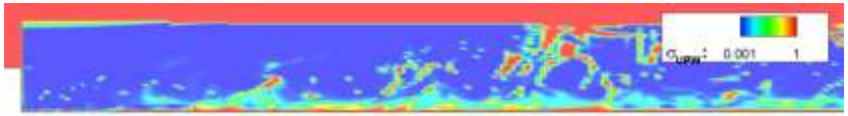

- Enhanced SA DDES (Strelets et al., 2014);
- Hybrid CD/UPW* method (Travin et al., 2004) based on EBR higher accuracy scheme

*pure CD scheme is unstable

Verification

Test case #3: Turbulent flow in channel with back facing step

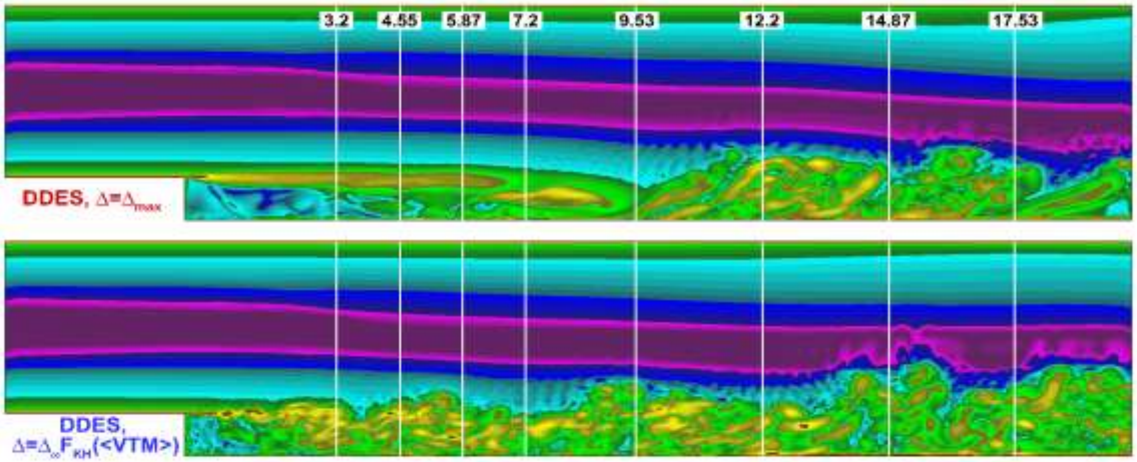

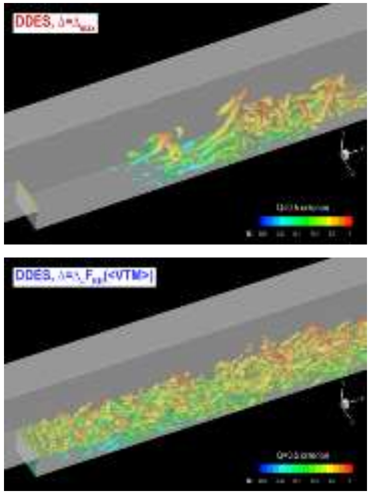

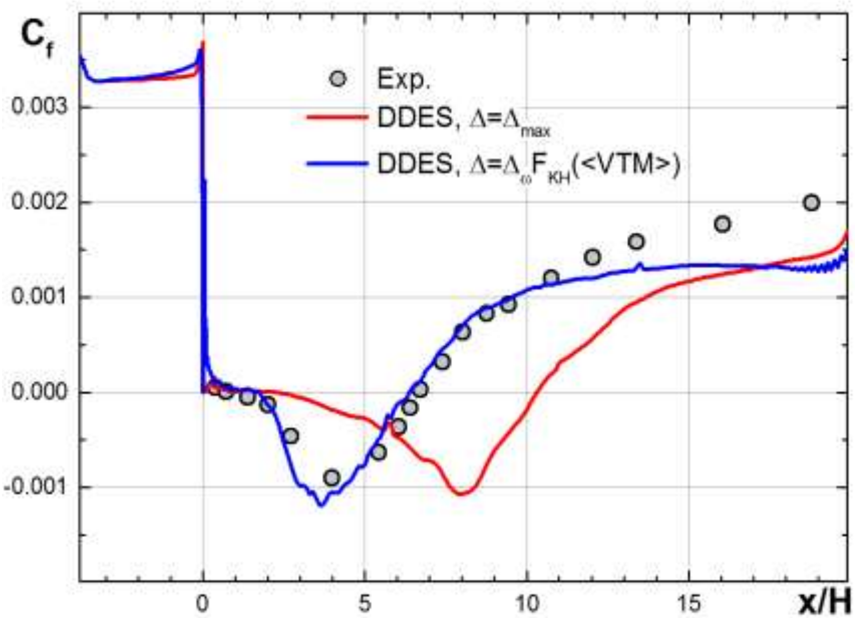

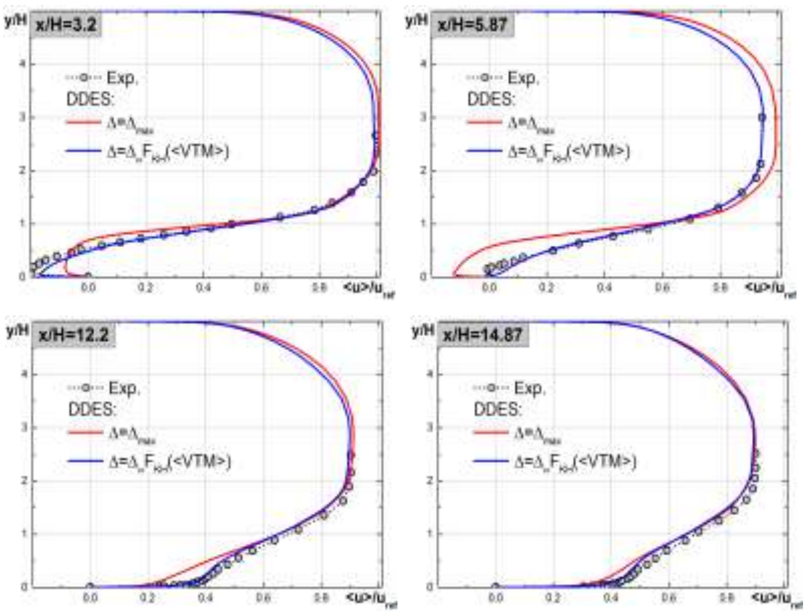

Introduction

EBR and WENO-EBR Schemes

In-House Code NOISEtte

Verification

Simulations

Problem #1
Transonic flow over the wedge-shaped body with backward-facing step

Experimental setup (by TsNIIMash)

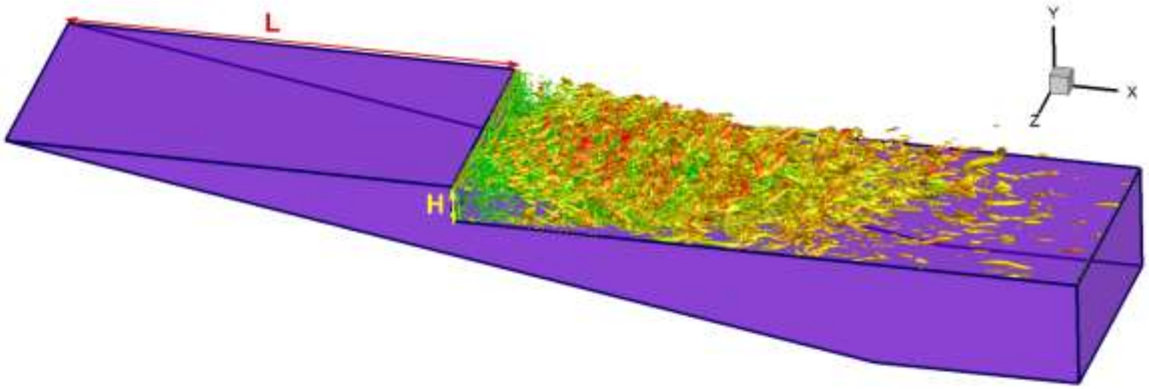

Flow parameters:
Re_L = **7.2·10^6**
M_∞ = **0.913**
L = 0.358 [м]

Flow peculiarities:

- transonic flow self-rebuiling: flow structure rebuilding, increasing of OASPL
- interfering separation-induced flows in the base region

Experimental data:

- shadowgraphs;
- streamtraces on surfaces;
- profies of C_p • OASPL • PSD(p')

Objectives:

- verification of numerical methods;
- Investigation of the peculiarities and the physics of the flow

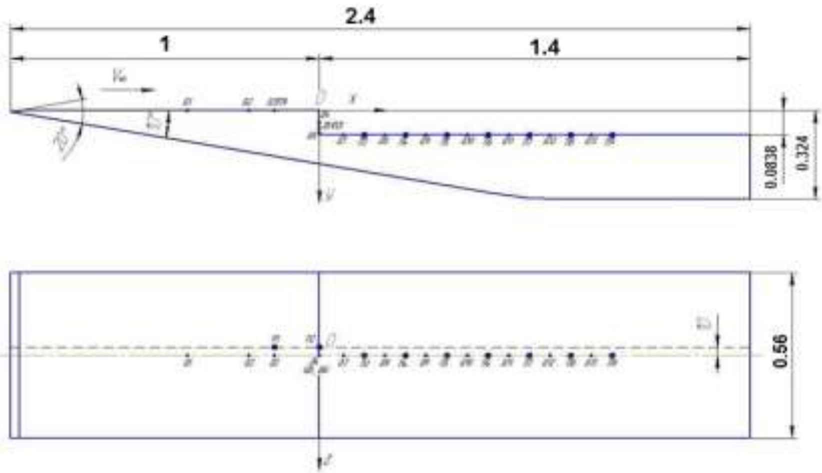

Simulations: Problem #1

Computational setup

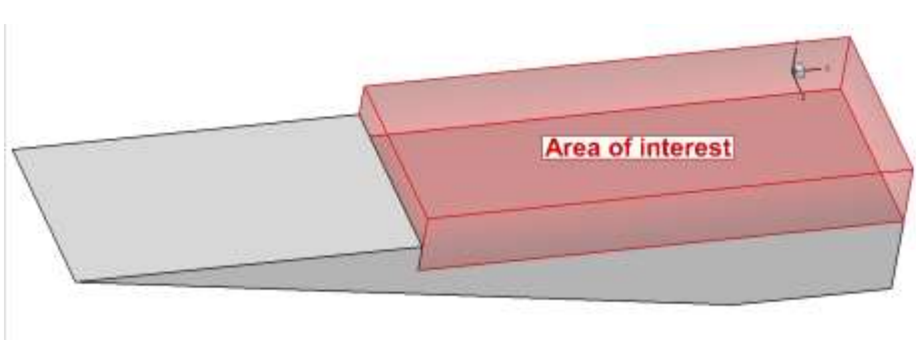

- Approach: SA RANS, SA IDDES;
- Numerical scheme: hybrid EBR WENO-CD/UPW

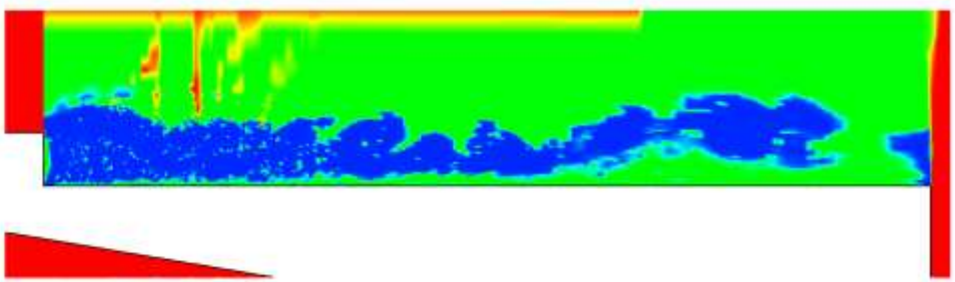

Red: WENO-EBR

Blue-green: CD/UPW*

$\sigma_{\text{upw}}^{\max} = 0.5$ in the area of interest

- Time integration: implicit 2nd order scheme. CFL<1 in the (LES) region of interest
- Mesh: 26M nodes, 149M tetrahedrons, spanwise resolution: $\Delta z = 2 \cdot 10^{-3} \cong \delta / 6$
- Modification of LES sub-grid scale:

$\Delta = \max\left(\Delta x, \Delta y, 0.1\Delta z\right)$ in the region $0 \le x \le 2H$

*[Travin et al., 2004]

Simulations: Problem #1

Visualization: turbulent structures

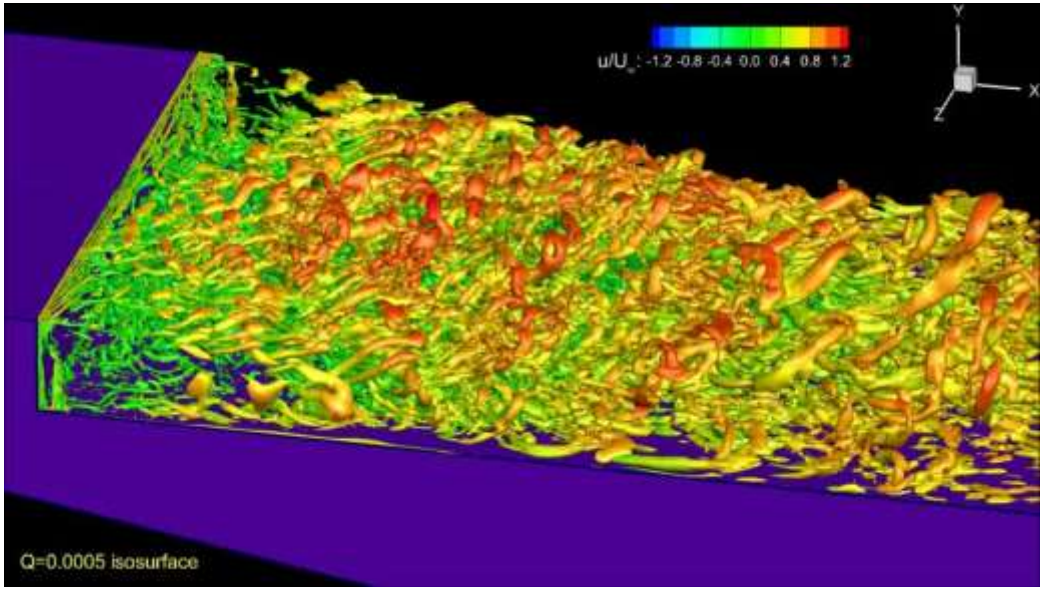

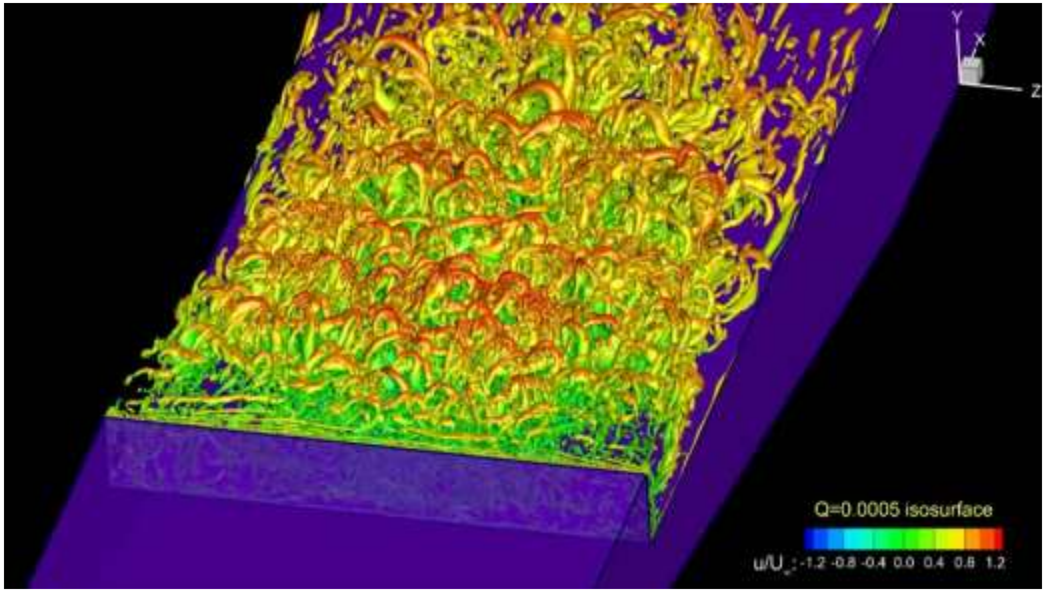

Visualization: acoustics

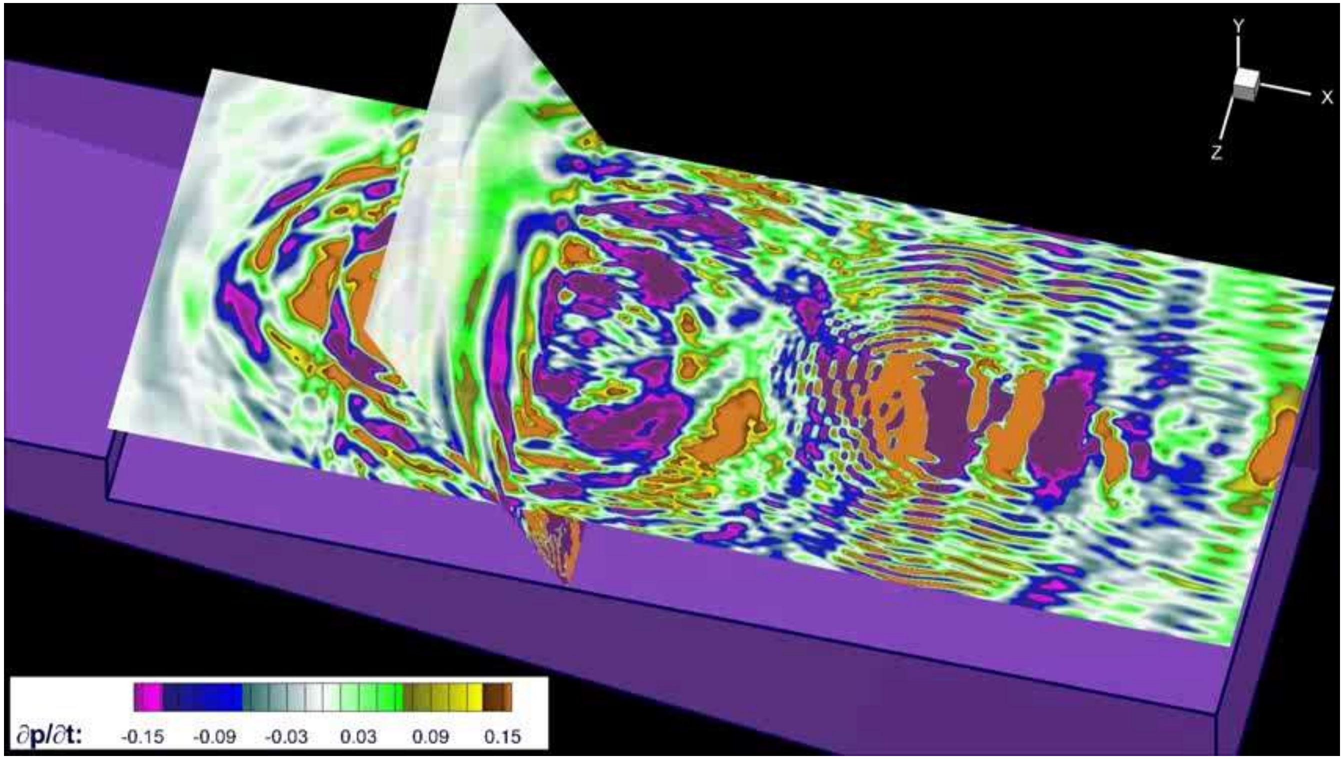

Verification: mean flow

Visually recirculation zone is predicted correctly

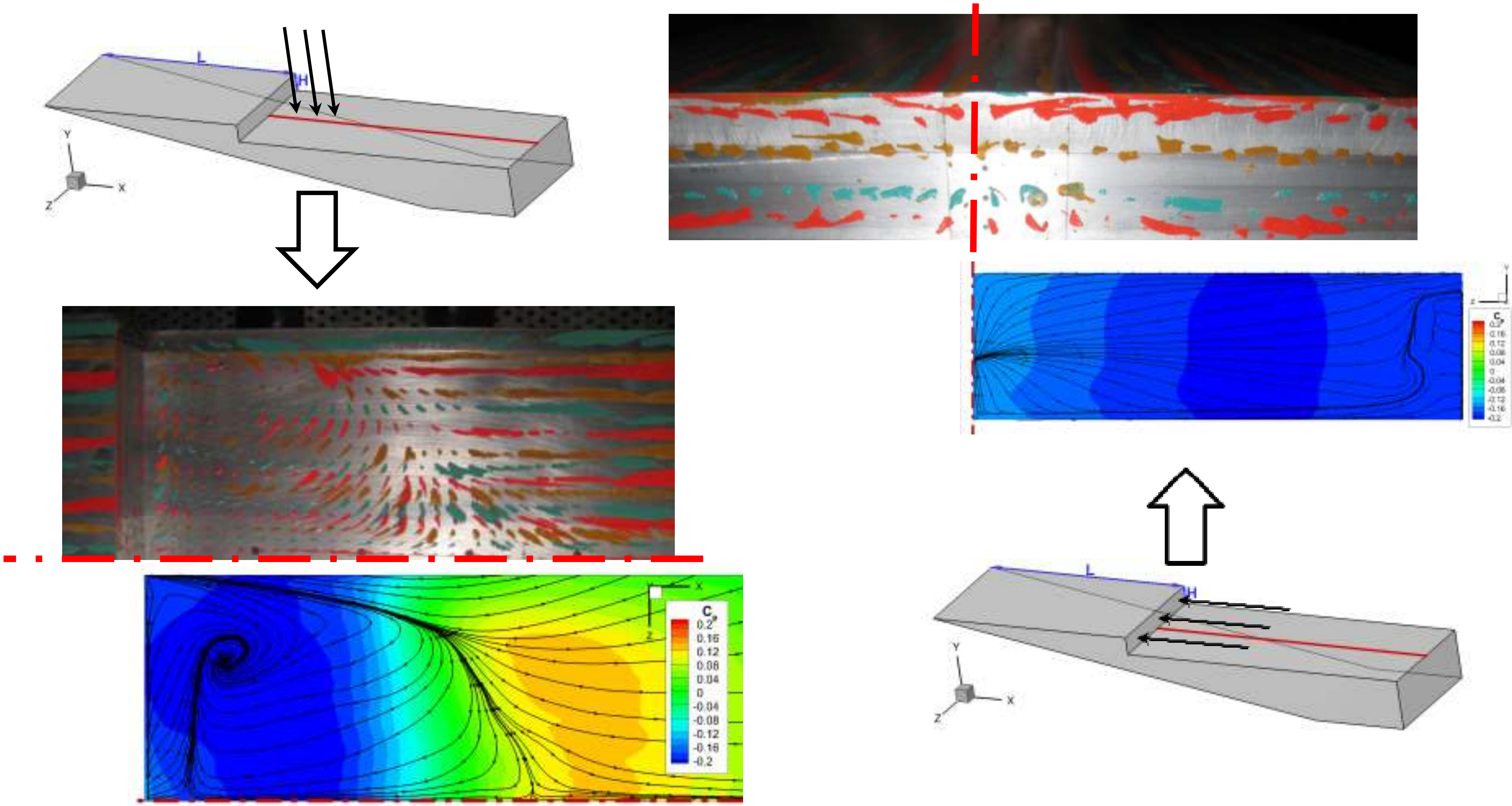

Verification: mean flow profiles

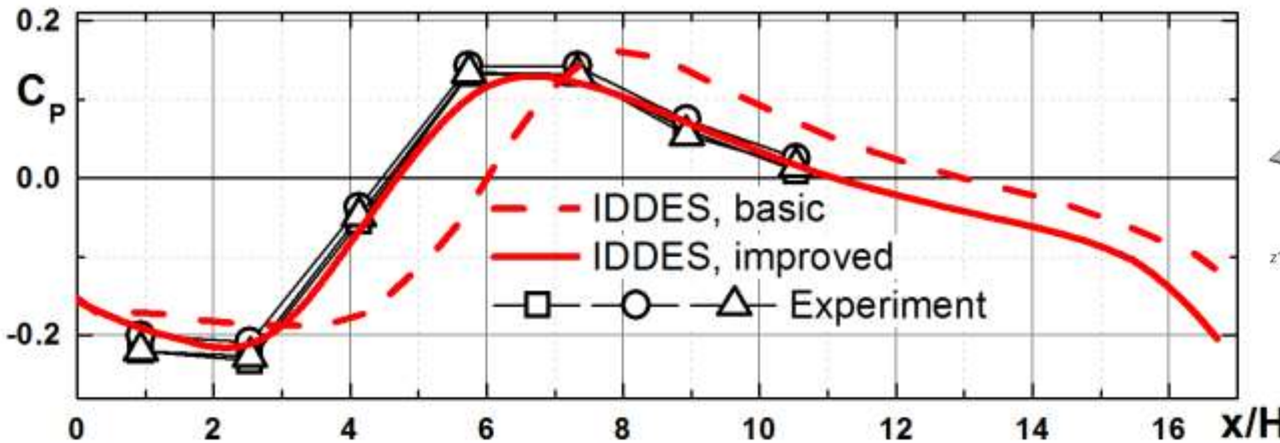

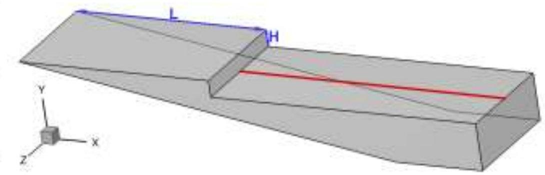

Good agreement with experiment

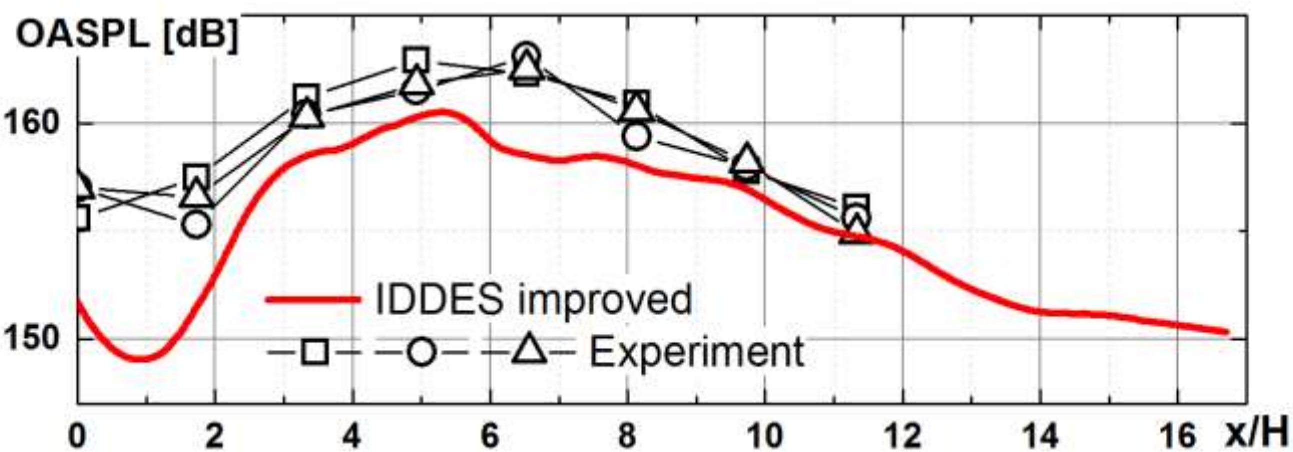

Acceptable agreement with experiment on average pressure fluctuations level

The difference can be explained by contribution of small-scales high-frequency turbulent pulsations considered at experimental levels and are not resolved in the simulation

Problem #2
Flow near tandem of square cylinders

Objective: investigation of noise generation mechanisms near landing gears

- **EU FP7 VALIANT project**
- Experiment: NLR, Netherlands
- Computational setup: SA DDES, EBR scheme
- Mesh: 12.5M nodes, 73M tetrahedrons

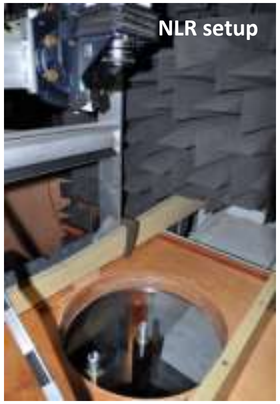

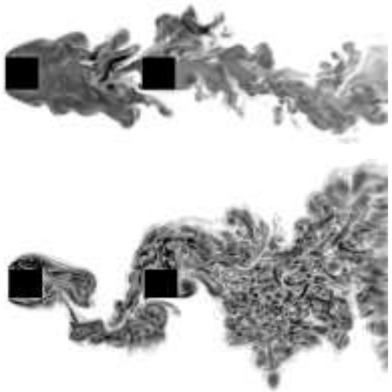

Comparison with the experimental data:

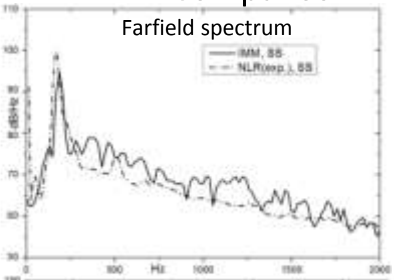

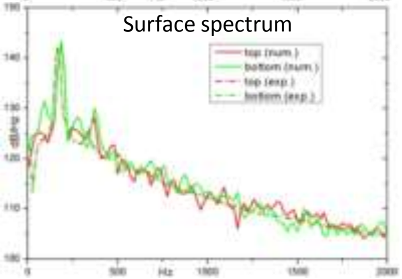

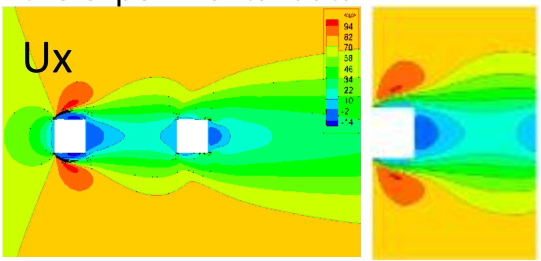

Расчет Эксперимент (PIV)

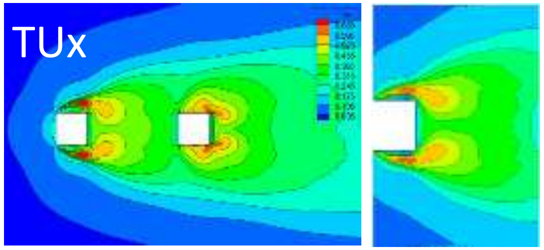

Good agreement with experimental data, also on acoustics

Problem #3
Numerical prediction of aerodynamic and aeroacoustic characteristics of axisymmetric flow generated by shrouded tail rotor

Objective: to evaluate aerodynamic and acoustic characteristics of ducted rotor for various rotor angular velocity and various pitch angles of rotor blades using inviscid-flow approach

Problem formulation

11-blade tail rotor in ring

Rotor radius — 0.7 м

Upstream flow velocity: $V = 0\,\text{m/s}$

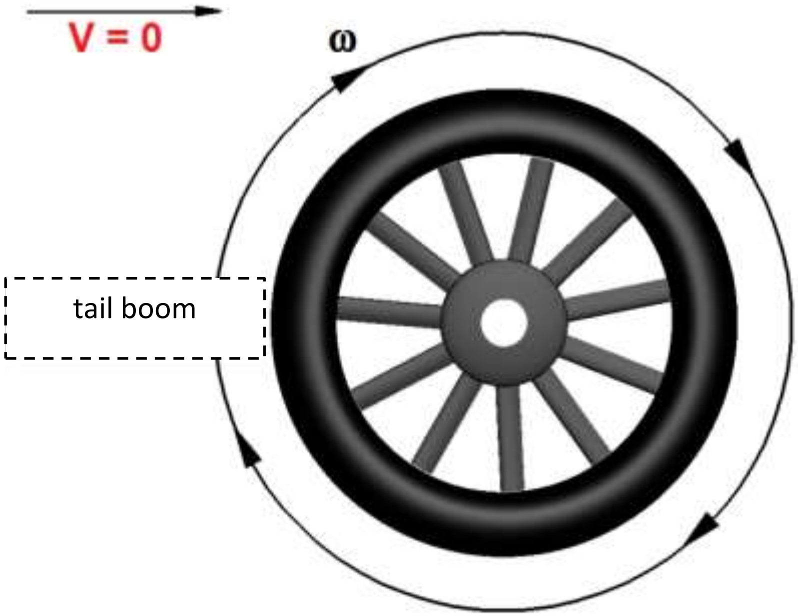

1. Zero upstream velocity

⇩

Axial symmetry

⇩

1) Simulation of single-blade in a 32.72º sector
2) Periodic boundary conditions in the azimutal direction

	1 mode	2 mode
Rotation frequency	$f = 46.6\,\text{Hz}$	$f \approx 40.926\,\text{Hz}$
Angular velocity	$\omega = 292.80\,\text{rad/s}$	$\omega \approx 257.14\,\text{rad/s}$
Blade tip velocity	$V_{tip} \approx 205\,\text{m/s}$	$V_{tip} = 180\,\text{m/s}$

Simulations: Problem #3

Geometry, Computational domain, Boundary Surfaces

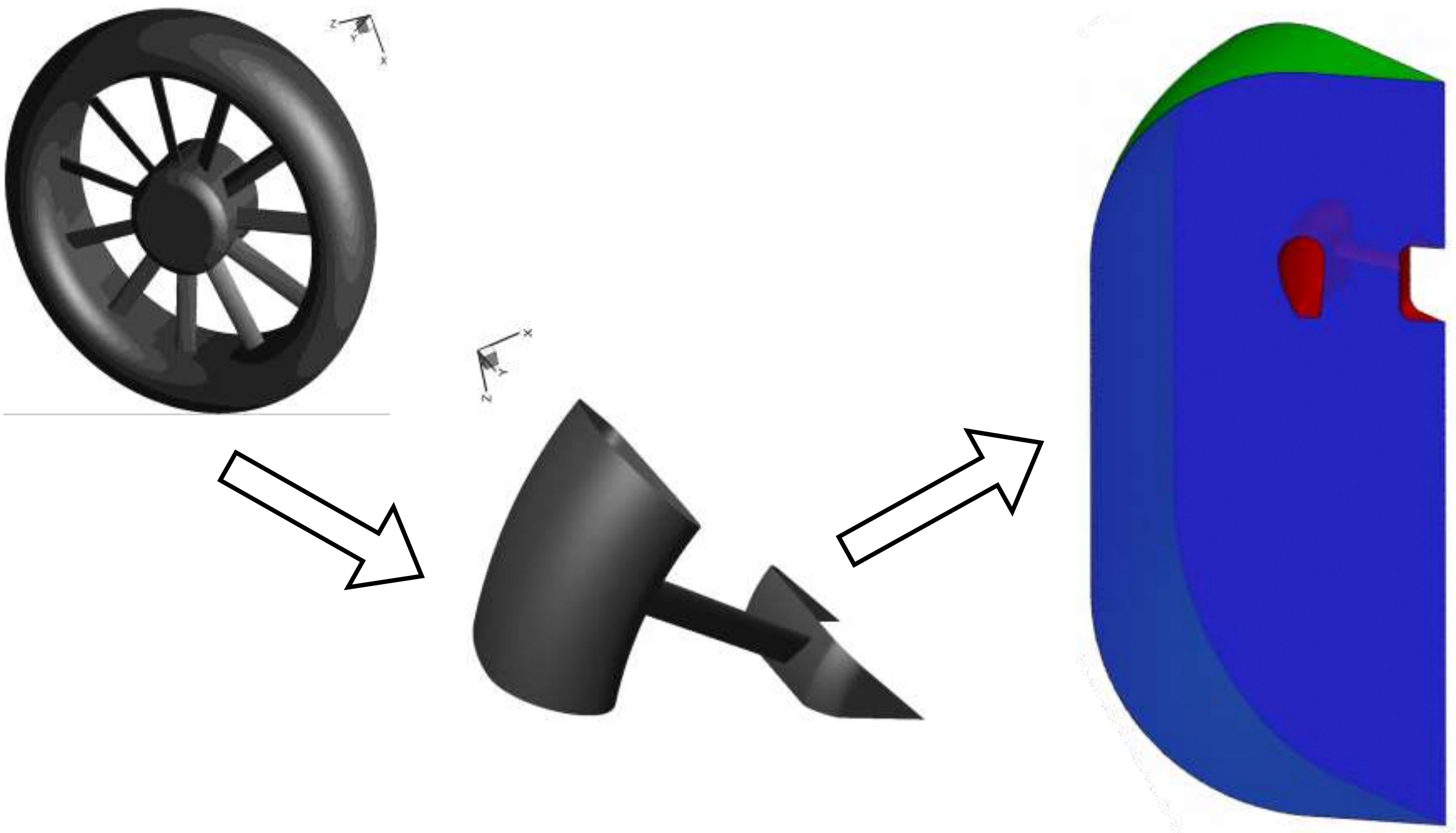

Mathematical model:

Euler equations
in a non-inertial rotating frame of reference

$$\mathbf{V} = \boldsymbol{\omega} \times \mathbf{r}$$

$$\frac{\partial \rho}{\partial t} + \operatorname{div} \rho (\mathbf{u} - \mathbf{V}) = 0$$

$$\frac{\partial \rho \mathbf{u}}{\partial t} + \operatorname{Div} \rho (\mathbf{u} - \mathbf{V}) \otimes \mathbf{u} + \nabla p = -\rho (\boldsymbol{\omega} \times \mathbf{u})$$

$$\frac{\partial E}{\partial t} + \operatorname{div} (\mathbf{u} - \mathbf{V}) E + \operatorname{div} \mathbf{u} p = 0$$

Mesh:

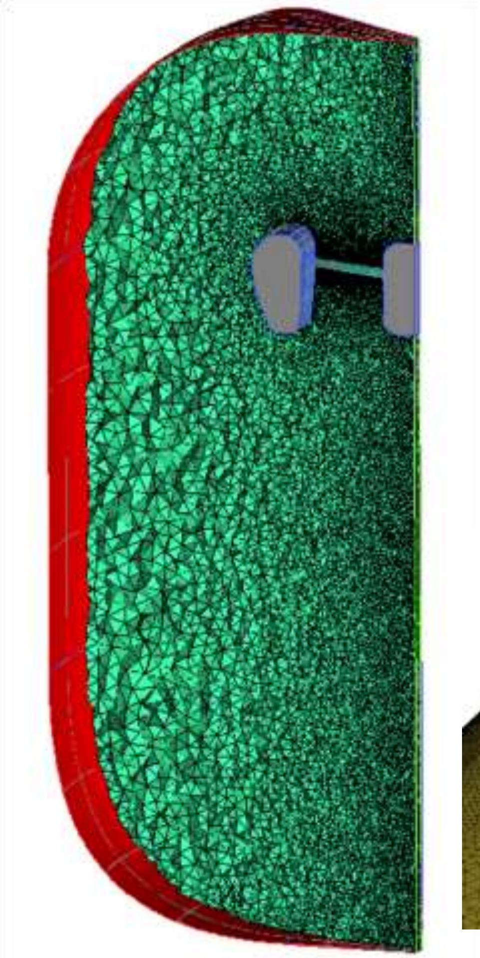

Number of nodes:

2.3-2.7 млн

Number of tetrahedra:

13.6-15.2 млн

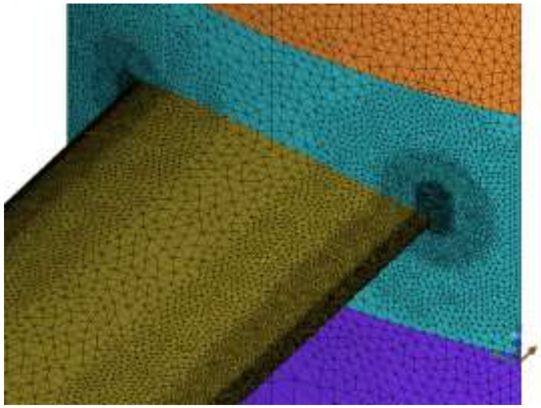

Simulations: Problem #3

Numerical results: flow pattern

Steady flow
after 10 cycles

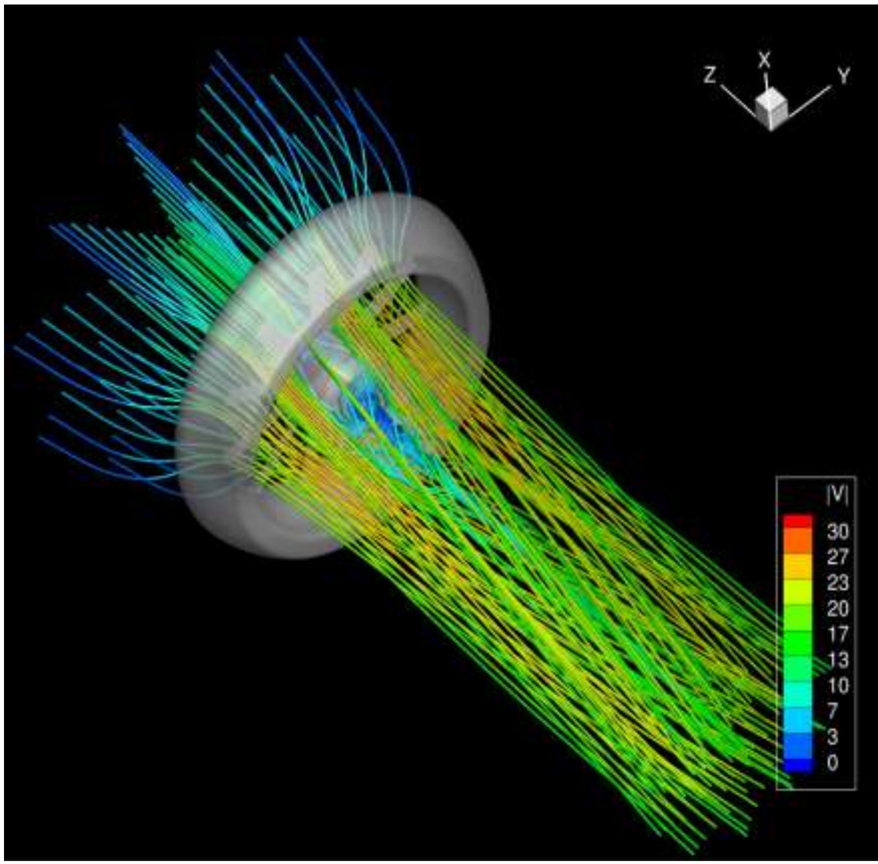

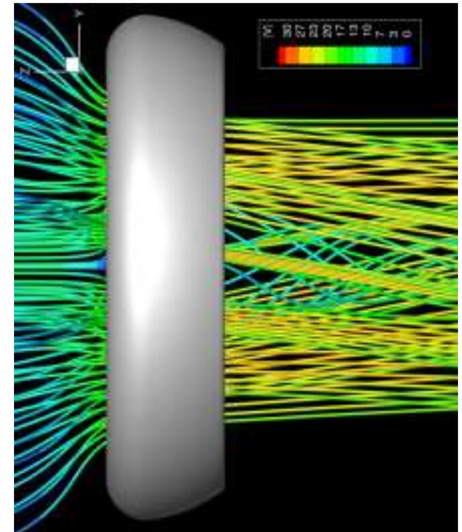

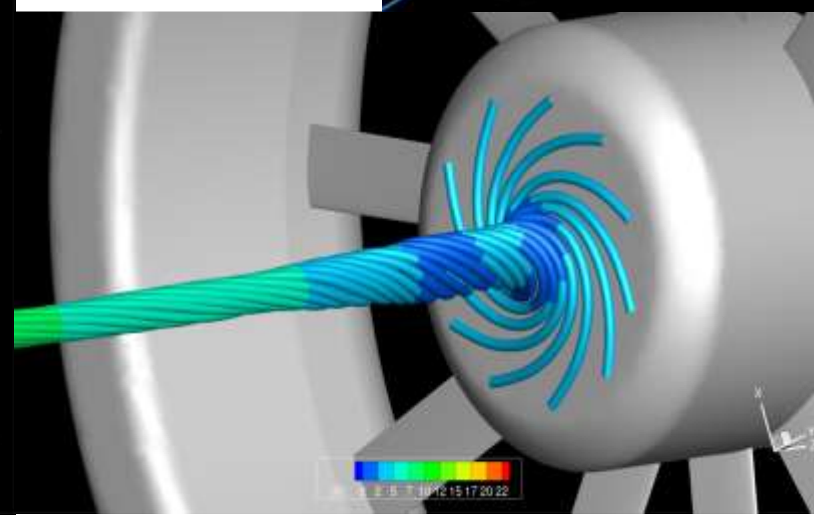

Streamtraces colered by velocity magnitude

Aerodynamic forces

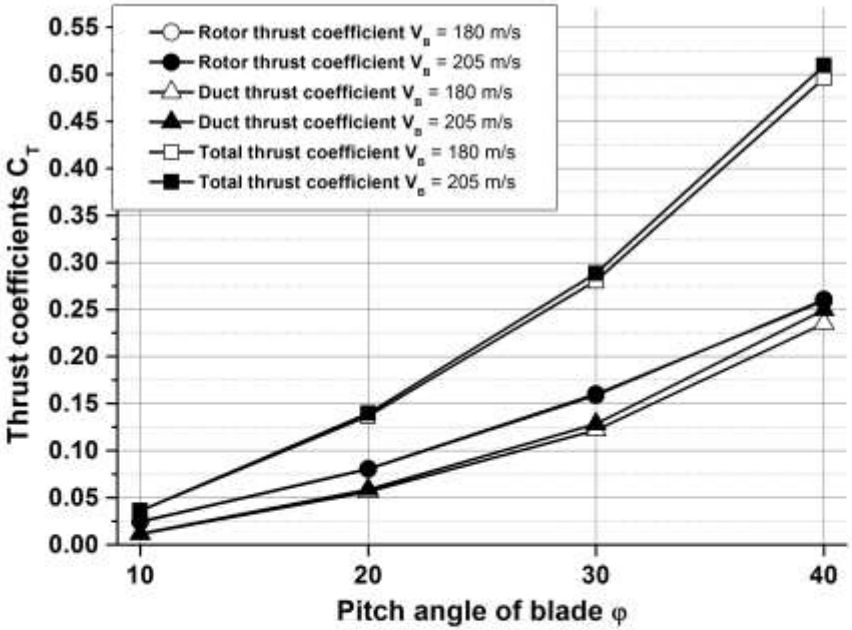

Rotor, ring and total thrust coefficients

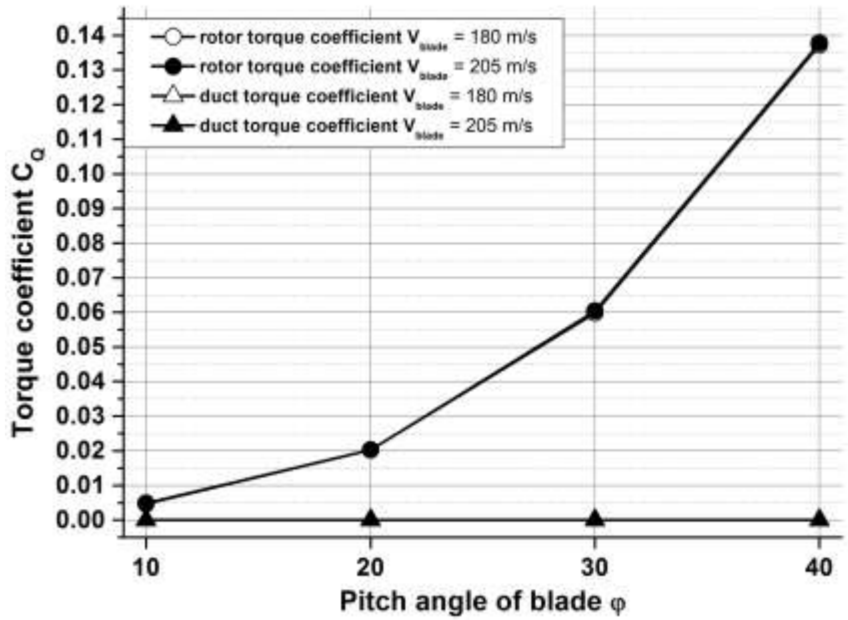

Rotor, ring torque coefficient

There is no experimental data. **The correctness of the simulations is confirmed by the self-similarity of solution at different blade tip velocities.**

Simulations: Problem #3

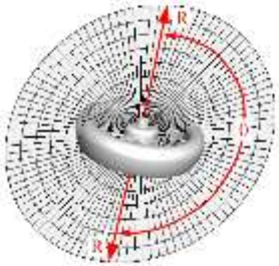

Far field pressure pulsations

FW-H: Directivity diagram depending on control surface

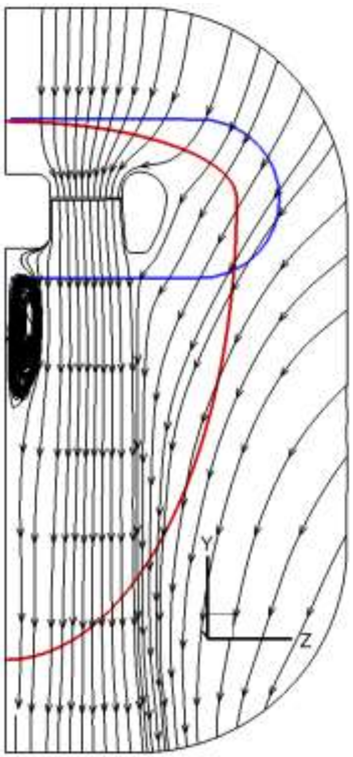

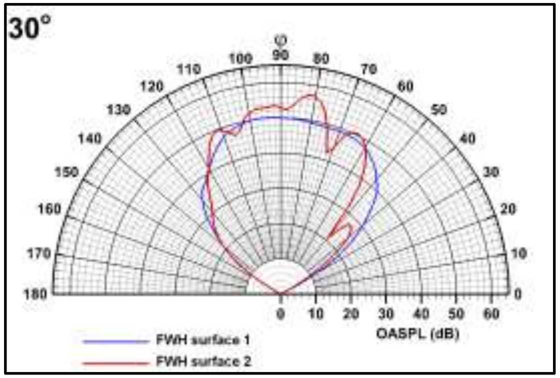

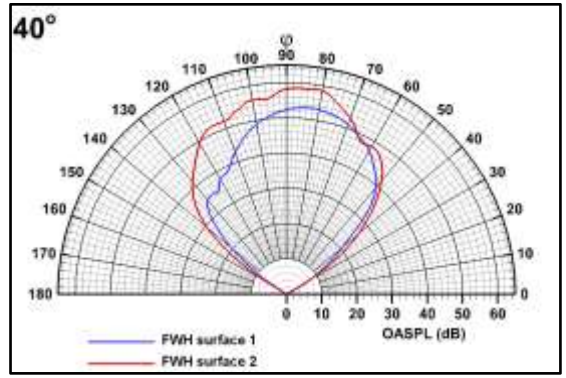

$$V_{tip} = 205\,\mathrm{m/s}$$

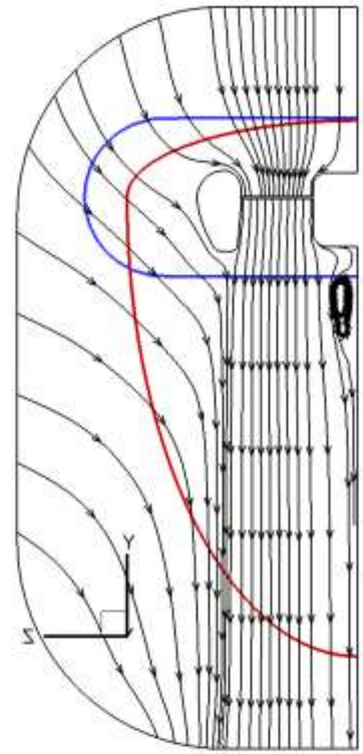

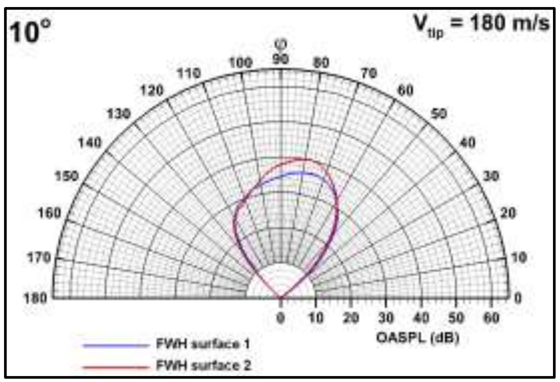

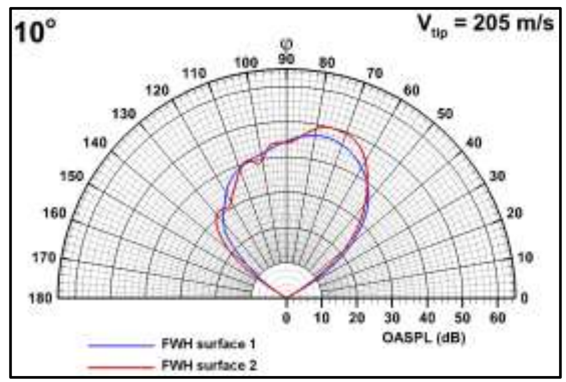

Overall Sound Pressure Level (**OASPL**) at the distance 150m

Thank you for attention!